Structural investigation of Fe silicide films grown by pulsed laser deposition

O. P. Karpenko, C. H. Olk,[a] and S. M. Yalisove
University of Michigan, Department of Materials Science and Engineering, 2300 Hayward Street, Ann Arbor, Michigan 48109-2136

J. F. Mansfield
University of Michigan, Electron Microbeam Analysis Laboratory, 2455 Hayward Street, Ann Arbor, Michigan 48109-2143

G. L. Doll
North American Operations Research and Development Center, General Motors Corporation, Warren, Michigan 48090-9055

(Received 24 March 1994; accepted for publication 25 April 1994)

Pulsed laser deposition was used to grow epitaxial β-$FeSi_2$ films on Si(111) (1×1) and Si(111) (7×7) with the following epitaxial orientations: β-$FeSi_2$(001)//Si(111) with β-$FeSi_2$[010]//Si⟨110⟩ and three rotational variants. Silicide growth was influenced by substrate temperature and deposition rate, but not by the structure of the starting surface. Films containing both β-$FeSi_2$ and FeSi were formed at low substrate temperatures and high deposition rates, while films containing only β-$FeSi_2$ were formed at higher substrate temperatures and lower deposition rates. FeSi grains had the following epitaxial relationship to the Si substrate, FeSi(111)//Si(111) with FeSi($\bar{1}$10)//Si(11$\bar{2}$). The microstructure of the silicide films varied with film thickness, as did the roughness at the silicide/Si interface. These results suggest that an Fe-rich environment was created during the growth of the silicide films.

I. INTRODUCTION

Semiconducting β-$FeSi_2$ has received a great deal of attention due to its electrical properties and compatibility for growth on Si substrates. β-$FeSi_2$ exhibits a direct electrical transition with a band-gap energy of 0.87 eV ($\lambda \approx 1.42$ μm).[1,2] This energy corresponds to a wavelength of light which lies within the optimal range for use with fiber optic lines and makes β-$FeSi_2$ an ideal material for the fabrication of optoelectronic devices. In addition, β-$FeSi_2$ has an orthorhombic structure ($a=9.86$ Å, $b=7.79$ Å, $c=7.83$ Å) with several planes well matched to and suitable for epitaxial growth on Si(100) and Si(111) surfaces. Given these materials properties, the use of β-$FeSi_2$ could possibly lead to the integration of optoelectronic devices with existing Si technology.

Previously, epitaxial β-$FeSi_2$ has successfully been grown on Si(100)[3] and Si(111)[4–8] using a variety of growth techniques including solid phase epitaxy (SPE),[4,5] molecular beam epitaxy (MBE),[7] liquid phase epitaxy,[8] and ion beam synthesis.[6] Currently, the films with the highest structural quality have been grown by SPE and MBE using a template technique.[7] Unfortunately, these films are not suitable for the fabrication of devices due to high defect densities and small domain sizes. In order to overcome these difficulties, more work in optimizing the growth process, or the use of other deposition techniques will be needed.

Recently, epitaxial β-$FeSi_2$ was successfully grown on Si(111) using pulsed laser deposition (PLD).[9] The use of PLD offers several advantages over the use of other deposition techniques. It does not involve multiple step deposition procedures, as does the template technique, nor does it require a large thermal budget in order to affect mass transport over long distances, as does SPE. In addition, PLD can offer precise control over the final film composition. Previous studies have shown that the stoichiometry of PLD films is identical to that of the ablation target in many materials systems.[10,11] The quality of the β-$FeSi_2$ films fabricated by PLD may also be affected by the higher kinetic energies of the ablated flux, as well as by the various chemical species which could be produced during the ablation process.[11,12] This study focuses on the structural characterization of Fe silicide films grown by PLD on both Si(111) (1×1) and reconstructed Si(111) (7×7) surfaces.

II. EXPERIMENT

Fe silicide films were grown on both Si(111) (1×1) and reconstructed Si(111) (7×7) surfaces using a PLD system in a load-locked ultrahigh vacuum growth chamber with a base pressure of 2×10^{-10} Torr. High resistivity, $\rho > 10$ kΩ cm, p-type Si(111) wafers were dipped in a dilute HF solution ($HF:H_2O=1:20$) for 5 min in order to remove the native silicon oxide and passivate the surface by hydrogen termination.[13] Wafers were then rinsed in de-ionized water and mounted onto a Mo substrate holder before being introduced into the deposition system via loadlock. The substrates were positioned 7 cm in front of the deposition target in the growth chamber. After introduction into the growth chamber and prior to heating, substrates were examined using reflection high-energy electron diffraction (RHEED) with a 15 keV electron beam aligned along a Si⟨110⟩ direction. In all cases, RHEED revealed streaked (1×1) surface diffraction patterns, typical of hydrogen terminated Si(111) (1×1) surfaces. Heating the Si substrates above the hydrogen desorp-

[a]North American Operations Research and Development Center, General Motors Corporation, Warren, MN 48090-9055.

 0021-8979/94/76(4)/2202/6/$6.00

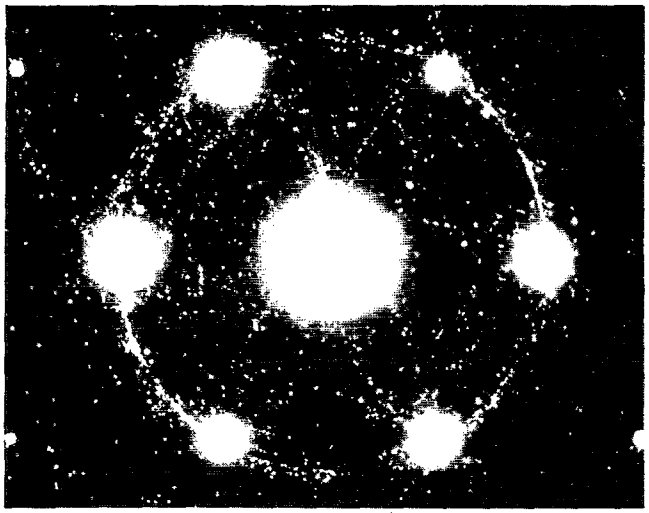

(a)

(b)

FIG. 1. (a) Plan-view TED pattern near the Si(111) zone axis for a Fe silicide film grown by deposition of Fe and annealing on Si(111). (b) Plan-view transmission electron micrograph near the Si(111) zone axis for a 490 Å film grown by deposition of Fe on Si(111) (7×7) followed by annealing to 600 °C.

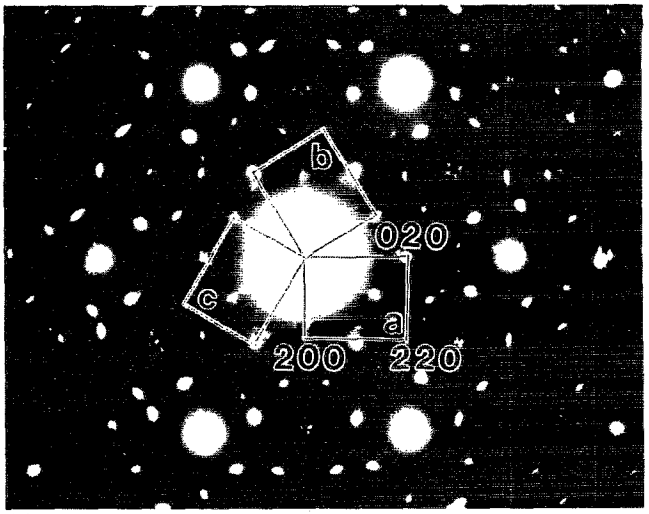

(a)

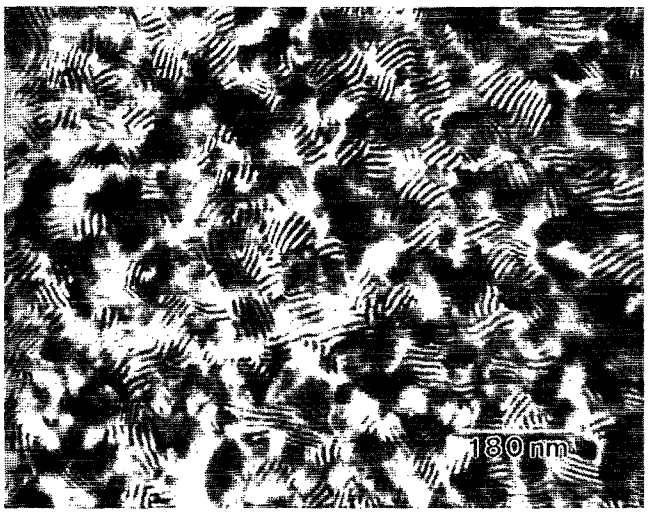

(b)

FIG. 2. (a) Plan-view TED pattern near the Si(111) zone axis for a β-$FeSi_2$ film grown by pulsed laser deposition from a stoichiometric $FeSi_2$ target on Si(111). The letters a, b, and c denote the three rotational variants of β-$FeSi_2$ on Si(111). (b) Plan-view bright-field TEM micrograph near the Si(111) zone axis for a 150 Å film, containing only β-$FeSi_2$, grown by deposition from a stoichiometric $FeSi_2$ target on Si(111) (1×1).

tion temperature did not result in reconstructed surfaces, suggesting the presence of surface contaminants. Reconstructed Si(111) (7×7) surfaces were prepared by heating the substrate to 820 °C and annealing for ≈10 min while depositing Si by PLD from a Si target at a slow rate to a total thickness of ≈15 Å. This procedure consistently produced reconstructed Si(111) (7×7) surfaces as evidenced by streaked (7×7) RHEED patterns. Substrates were heated with a heating coil located in the back of the substrate holder. Temperatures were calibrated against an optical pyrometer and a thermocouple attached to the substrate holder.

After preparing the Si surfaces for growth, the substrates were brought to the growth temperature and depositions were performed. Light from a KrF excimer laser (λ=248 nm) was focused through a quartz window onto the ablation target at an incidence angle of 45°. The incident laser beam produced a flux of ablated material which was highly forward directed toward the substrate. During PLD, the angular distribution of the flux typically follows a $\cos(\theta)^n$ dependence, where θ denotes the take-off angle of the ablated material relative to the target normal, and n can vary from 8 to 12 depending on target and beam conditions.[14] Currently, work is in progress to characterize the angular distribution, energy distribution, and chemical composition of the ablated flux produced in our system.[15] The energy and pulse rate of the incident laser beam (300–500 mJ per pulse and 1–2.5 Hz, respectively) were varied to give an effective deposition rate varying from 0.03 to 0.11 Å/s. The laser beam was rastered across the target surface in order to prevent pitting of the target.

In an attempt to grow epitaxial β-$FeSi_2$, two deposition schemes were used. The first scheme involved deposition of

pure Fe onto a Si wafer followed by annealing. Wafers were held nominally at room temperature during deposition and were annealed to 550–650 °C in order to form Fe silicide by an SPE reaction. Films prepared by this method ranged in thickness from 490 to 900 Å. The second scheme involved congruent deposition of Fe and Si from a stoichiometric $FeSi_2$ target onto a heated wafer, T=500–630 °C. Films prepared by this method were grown to a thickness varying from 75 to 1200Å. Both deposition schemes were attempted on Si(111) (1×1) and Si(111) (7×7) surfaces. During deposition, the pressure did not exceed 1×10^{-9} Torr.

Structural characterization of all films was performed using both a Phillips 420 T and a JOEL 4000 EX transmission electron microscope operating at 120 and 400 kV, respectively. Plan-view samples were prepared by ultrasonic cutting, mechanical thinning to ≈125 μm, and chemical etching to perforation. Cross-section samples were prepared by substrate cleavage, mechanical thinning to ≈30 μm, polishing and ion milling to perforation with 5 keV Ar^+ ions.

III. RESULTS

A. Deposition from an Fe target and annealing

The Fe silicide films fabricated by PLD of pure Fe and annealing did not grow epitaxially on either the Si(111) (1×1) or the reconstructed Si(111) (7×7) surfaces. Initially, the deposition of 150–300 Å of Fe onto unheated Si(111) surfaces resulted in spotted RHEED patterns characteristic of rough Fe films. These films were subsequently annealed to 550–650 °C. At the onset of annealing a complete loss of RHEED intensity was observed. Further annealing did not result in the reappearance of coherent RHEED patterns. Analysis of the films using transmission electron microscopy (TEM) indicated that the films were polycrystalline and had no apparent orientation to the substrate. Plan-view transmission electron diffraction (TED) patterns [Fig. 1(a)] showed discontinuous rings and suggested the presence of several Fe silicide phases including β-$FeSi_2$ and FeSi. Bright-field [Fig. 1(b)] and dark-field TEM revealed continuous arrays of highly defected grains with an average grain size of ≈500 nm. Neither varying the deposition conditions, nor changing the annealing parameters significantly affected the quality of these silicide films.

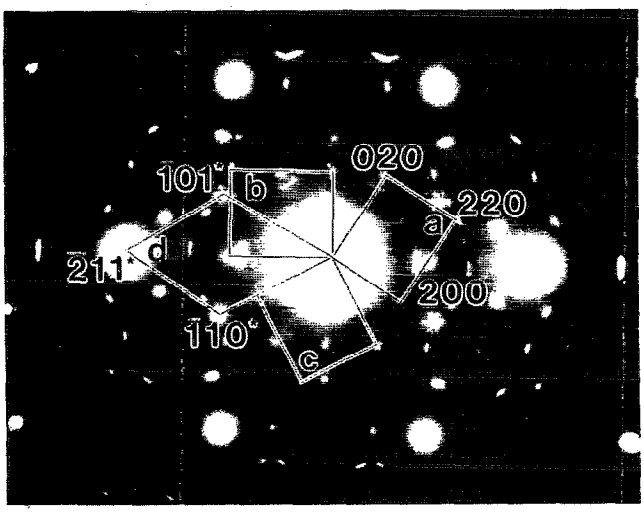

(a)

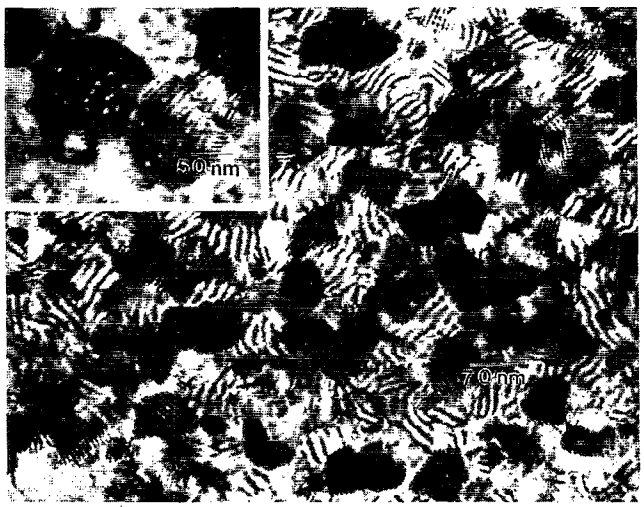

(b)

FIG. 3. (a) Plan-view TED pattern near the Si(111) zone axis for a film containing both β-$FeSi_2$ and FeSi, grown by pulsed laser deposition from a stoichiometric $FeSi_2$ target on Si(111). The letters a, b, c, and d denote the three rotational variants of β-$FeSi_2$ and the epitaxial orientation of FeSi on Si(111), respectively. (b) Plan-view bright-field TEM micrograph near the Si(111) zone axis of a 500 Å film, containing both β-$FeSi_2$ and FeSi, grown by pulsed laser deposition from a stoichiometric $FeSi_2$ target on Si(111) (1×1).

B. Deposition from an $FeSi_2$ target

Fe silicide films grew epitaxially on both Si(111) (1×1) and Si(111) (7×7) surfaces when fabricated by PLD from a stoichiometric $FeSi_2$ target. Analysis of plan-view TED patterns [Figs. 2(a) and 3(a)] showed that depending on the deposition conditions, the films contained either a single phase, β-$FeSi_2$, or two phases, β-$FeSi_2$ and FeSi. In all of the films, the following epitaxial relationships were identified:

β-$FeSi_2(001)$//Si(111) with β-$FeSi_2[010]$//Si$[\bar{1}01]$,

β-$FeSi_2(001)$//Si(111) with β-$FeSi_2[010]$//Si$[01\bar{1}]$,

β-$FeSi_2(001)$//Si(111) with β-$FeSi_2[010]$//$[1\bar{1}0]$ [see Figs. 2(a) and 3(a)],

and

FeSi(111)//Si(111) with FeSi$[\bar{1}10]$//Si$[11\bar{2}]$ [see Fig. 3(a)].

Further analysis of the TED patterns showed that nearly all of the diffraction maxima could be accounted for by considering either single scattering events or multiple scattering events from Si, FeSi and/or β-$FeSi_2$. The multiple scattering events were a result of double diffraction of the electrons from various Si, FeSi, and β-$FeSi_2$ planes. One example of double diffraction is easily seen in the TED patterns of the two phase films [Fig. 3(a)]. In addition to diffraction maxima corresponding to single scattering events from FeSi, distinct satellite diffraction spots (hexagonal arrays) were seen around each of the 110 type FeSi diffraction maxima. These satellites were formed by double diffraction of the transmitted electron beam from the FeSi(110) and the Si(220) families of planes.

The presence of FeSi in the β-$FeSi_2$ films was dependent on both substrate temperature and deposition rate. For growth on Si(111) (1×1) surfaces, the two phase films were formed at low substrate temperatures, 500–530 °C, and a deposition rate of ≈0.09 Å/s, while single phase films were formed at higher substrate temperatures, ≥570 °C, and a lower deposition rate, ≈0.03 Å/s. A similar behavior was observed for growth on reconstructed Si(111) (7×7) surfaces. All of these films were grown at temperatures ≥570 °C and contained mostly β-$FeSi_2$. Growth performed at a deposition rate of ≈0.03–0.04 Å/s produced two phase films with very small amounts of FeSi, <5%. These results are summarized in Table I.

Bright-field and dark-field TEM showed that the continuity of the films varied with film thickness. At low film thicknesses, the films were discontinuous and contained islands of tightly packed grains. As the film thickness was increased above ≈500 Å, continuous films were formed. The grain sizes in these films were determined directly from both bright-field and dark-field transmission electron micrographs, and were found to be approximately equal to the film thickness. β-$FeSi_2$ grains ranged in size from 150 to 950 Å for films 150–1200 Å thick. Bright-field TEM also revealed the presence of moiré fringes in the grains, indicating that the films were strain relieved to the bulk lattice parameter [see Fig. 2(b)]. Micrographs from the single-phase silicide films contained one predominant type of moiré pattern, a twofold symmetric pattern with a wide fringe spacing, and three variants rotated ~120° from one another [see Fig. 2(b)]. The spacing in the moiré fringes, as seen in the bright-field micrographs, measured ≈130 Å and corresponded well to the spacing which was calculated[16] for the interference from the Si(220) and β-$FeSi_2$(040) families of planes:

$$d_{\text{moiré}}=\frac{d_{\text{Si(220)}}\times d_{\beta\text{-FeSi}_2\text{(040)}}}{d_{\text{Si(220)}}-d_{\beta-\text{FeSi}_2\text{(040)}}}=135\ \text{Å}.$$

In addition to the wide-band moiré patterns seen in the single-phase films, sixfold symmetric moiré patterns were observed in the two phase films [see Fig. 3(b)]. The fringe spacing in these sixfold symmetric moiré patterns measured ≈40 Å and agreed with the spacing which was calculated for the interference from the Si(220) and FeSi(112) families of planes, 39 Å. No significant difference was seen in the TEM analysis of films grown on Si(111) (1×1) and Si(111) (7×7).

Cross-section TEM showed that the roughness at the β-$FeSi_2$/Si(111) interface varied from film to film [see Figs. 4(a) and 4(b)] but stayed within a range of ≈80–120 Å. In all of the films, a large number of silicide grains had penetrated the Si substrate.

IV. DISCUSSION

A. Deposition from an Fe target and annealing

The poor epitaxial quality of the Fe silicide films formed by pulsed laser deposition of Fe followed by annealing is likely the result of inhibited mass transfer of Fe and Si across the silicide/Si interface and in the bulk of the film. As shown in previous studies, the epitaxial quality of β-$FeSi_2$ grown by SPE degrades above a predeposited Fe thickness of ≈90 Å (≈300 Å β-$FeSi_2$).[4] This breakdown in epitaxial quality is not yet fully understood. However, it is known that the type and sequence of chemical reactions which occur during the formation of β-$FeSi_2$ by SPE vary with the thickness of the predeposited Fe layer. For films with an initial Fe thickness <30 Å, the cubic FeSi and γ-$FeSi_2$ phases have been observed prior to their transformation into β-$FeSi_2$. For films with an initial Fe thickness >30 Å, the formation of an amorphous phase has also been observed at the onset of annealing (T≈250 °C), prior to the nucleation of β-$FeSi_2$ (T≈450 °C).[4,7] In our study, a complete loss of diffraction intensity in RHEED patterns was observed at the onset of

TABLE I. Summary of results for films fabricated by deposition from an $FeSi_2$ target.

Starting surface	Phases present	$T_{\text{substrate}}$ (°C)	E_{laser} (mJ)	Pulse rate (Hz)	Deposition rate (Å/s)	Volume fraction FeSi (%)	Film thickness (Å)
Si(111)[a] (1×1)	β-$FeSi_2$ +FeSi	500–530	500	2	≈0.09	≈25±5	500–800
Si(111)[a] (1×1)	β-$FeSi_2$	570–630	300	1	≈0.03	<2	75–1200
Si(111) (7×7)	β-$FeSi_2$ +FeSi	570±10	360	1	≈0.04	<5	500
Si(111) (7×7)	β-$FeSi_2$	580±10	300	1	≈0.03	<2	800

[a]Corresponds to a series of films fabricated at various deposition conditions.

(a)

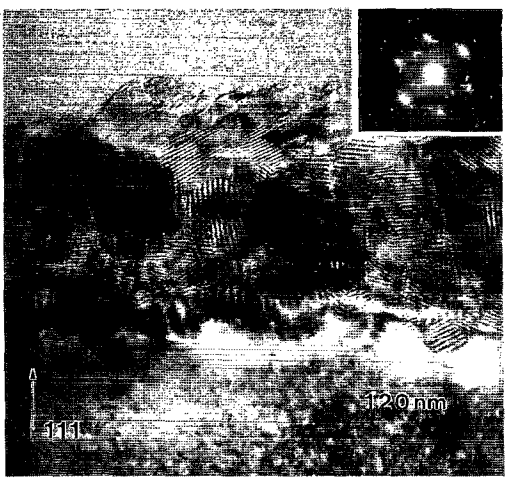

(b)

FIG. 4. (a) Cross-section TEM micrograph near the Si(110) zone axis for a 150 Å film, containing only β-$FeSi_2$, grown by pulsed laser deposition from a stoichiometric $FeSi_2$ target on Si(111) (1×1). (b) Cross-section TEM micrograph near the Si(110) zone axis for a 500 Å film, containing both β-$FeSi_2$ and FeSi, grown by pulsed laser deposition from a stoichiometric $FeSi_2$ target on Si(111) (1×1).

annealing, suggesting the formation of an amorphous layer. Further annealing did not result in the nucleation of epitaxial β-$FeSi_2$. Based on these observations we speculate that the formation of the thick amorphous layer inhibits mass transfer in the film, hence preventing the nucleation of an epitaxial film.

B. Deposition from an $FeSi_2$ target

Deposition from an $FeSi_2$ target resulted in the formation of either single phase, β-$FeSi_2$, films or two phase, β-$FeSi_2$ and FeSi, films. The presence of FeSi in the films grown at low temperatures and high deposition rates was confirmed by analysis of transmission electron diffraction patterns as well as by bright-field and dark-field TEM. Dark-field TEM images of the two-phase films, using $\vec{g}=110_{FeSi}$, have been used to measure the fractional area of the FeSi grains. This measurement served as a basis for an estimate of the volume fraction of FeSi in the Fe silicide films (see Table I). The presence of the FeSi phase is consistent with the results of previous studies in which the nucleation of epitaxial FeSi has been reported as an intermediate phase in the SPE growth of β-$FeSi_2$ films.[4]

TABLE II. Summary of the β-$FeSi_2$ epitaxial orientation for different film compositions.

Epitaxial orientation	Initial film composition	Method of deposition	References
β-$FeSi_2$(101)//Si(111)	≈100% Fe	SPE	4,5,7
	≈33% Fe	MBE	7
β-$FeSi_2$(001)//Si(111)	≈40% Fe	IBS,[a] MBE	6,7
β-$FeSi_2$(100)//Si(111)	≈40% Fe	MBE	7

[a]IBS is an acronym for ion beam synthesis.

Growth on the Si(111) (1×1) and reconstructed Si(111) (7×7) surfaces resulted in silicide films with similar epitaxial quality, compositions, and identical epitaxial orientations. This behavior suggests that the high kinetic energy of the incident flux resulted in either subplantation of the incident atoms or increased adatom mobility, hence reducing the influence of the surface structure on growth.

The β-$FeSi_2$ phase in all of the films grown on Si(111) exhibited the following epitaxial orientation: β-$FeSi_2$(001)// Si(111) with β-$FeSi_2$[010]//Si⟨110⟩ and three rotational variants. This epitaxial orientation results in a small lattice mismatch between the β-$FeSi_2$ and the Si substrate: +1.4% mismatch along Si⟨110⟩ and −1.2% mismatch along Si⟨112⟩.[7] The three rotational variants are a result of the differences in symmetry between the β-$FeSi_2$(001) epitaxial plane and the Si(111) surface plane. During growth, the twofold symmetric β-$FeSi_2$(001) plane (9.86 Å×7.79 Å rectangular mesh) aligns itself with the threefold symmetric Si(111) plane (3.84 Å triangular mesh) with the β-$FeSi_2$[010] direction of each variant parallel to a Si⟨110⟩ direction. Since there are three equivalent Si⟨110⟩ directions ($[\bar{1}01]$, $[01\bar{1}]$, and $[1\bar{1}0]$) rotated 120° from one another in the Si(111) surface plane, nucleation can occur independently in each of these orientations. The result is the formation of three rotational variants of β-$FeSi_2$.

The epitaxial orientation of β-$FeSi_2$ on Si(111) has previously been shown to be highly sensitive to the initial film composition (see Table II and below).[4–7] The most commonly observed epitaxial orientation is β-$FeSi_2$(101)// Si(111) with β-$FeSi_2$[010]//Si⟨110⟩. It has typically been seen for films fabricated by SPE[4,5,7] where the initial film composition was ≈100% Fe, as well as for films grown by MBE where Fe and Si were codeposited in a stoichiometric ratio, Fe:Si=1:2.[7] In addition, two other epitaxial orientations, β-$FeSi_2$(001)//Si(111) with β-$FeSi_2$[010]//Si⟨110⟩ and β-$FeSi_2$(100)//Si(111) with β-$FeSi_2$[010]//Si⟨110⟩, have been observed in films with an initial film composition of ≈40% Fe. The former orientation has been seen for films fabricated by MBE[7] and ion beam synthesis,[6] while the latter orientation has only been seen in films fabricated by MBE.[7]

Currently, the mechanisms by which the various epitaxial orientations nucleate have not been determined. Previous work has suggested two possible explanations for this behavior. One mechanism suggests that differences in the Gibbs free energy, associated with the transformation from the pseudomorphic precursor phases (FeSi with a CsCl structure or γ-$FeSi_2$ with a CaF_2 structure) to β-$FeSi_2$, lead to the

nucleation of different epitaxial orientations. The other possibility suggests that differences in the initial film composition result in different atomic interfacial structures at the precursor phase/Si interface. These interfacial differences may be responsible for the nucleation of β-$FeSi_2$ with the different epitaxial orientations.[7] A better understanding of these mechanisms could be instrumental in optimizing the growth of β-$FeSi_2$ films and may eventually lead to the fabrication of device quality material. Future studies should address the dependence of the β-$FeSi_2$ epitaxial orientation on film composition, specifically at the initial stages of growth.

The orientation of the PLD silicide films grown in the present study was β-$FeSi_2$(001)//Si(111) with β-$FeSi_2$[010]//Si⟨110⟩. Because this orientation has only been seen in films where the initial film composition was ≈40% Fe, it is likely that an initially Fe-rich environment was produced in the Si substrate. One possible explanation for the presence of the β-$FeSi_2$(001)//Si(111) epitaxial orientation is an Fe-rich flux incident on the substrate from the stoichiometric $FeSi_2$ target. An Fe-rich flux would create an initially Fe-rich film composition and could lead to the nucleation of silicide grains with the β-$FeSi_2$(001)//Si(111) epitaxial orientation. In addition, an Fe-rich flux would facilitate the formation of FeSi in low-temperature silicide films. However, results from a study of the PLD process used in the fabrication of these films indicates that the ratio of Fe to Si in the ablated flux is 1:2,[15] hence eliminating this possibility.

Another explanation for the presence of the β-$FeSi_2$(001)//Si(111) epitaxial orientation involves the shallow implantation or subplantation of Fe and Si from the flux into the Si substrate. Both the Fe and Si species produced in the ablation process have similar velocities, $v \approx 10^4$ m/s.[15] Since Fe has a higher mass than Si, it also has greater momentum and kinetic energy, resulting in deeper penetration into the substrate than Si.[13] This implantation of Fe would produce an Fe-rich environment within the Si substrate and could lead to the nucleation of β-$FeSi_2$ grains with an β-$FeSi_2$(001)//Si(111) epitaxial orientation. Currently work is in progress to better characterize the PLD process and to determine its effects on thin-film growth.[15]

V. SUMMARY

Single-phase β-$FeSi_2$ films with the following epitaxial orientations: β-$FeSi_2$(001)//Si(111) with β-$FeSi_2$[010]//Si⟨110⟩ and three rotational variants, have been grown on Si(111) using pulsed laser deposition from a stoichiometric $FeSi_2$ target. The monosilicide phase, FeSi, was also present with the following epitaxial orientation: FeSi(111)//Si(111) with FeSi[$\bar{1}$10]//Si[11$\bar{2}$]. This phase was only detected in films deposited at high deposition rates and low substrate temperatures. These data and the dependence of the β-$FeSi_2$(001)//Si(111) epitaxial orientation on initial film composition (Fe concentration ≈40%), suggest that this deposition technique creates a growth environment which is initially Fe rich. Work is in progress to characterize the PLD process used to fabricate the Fe silicide films.[15]

ACKNOWLEDGMENTS

The authors would like to thank David P. Adams and David J. Eaglesham for their helpful discussions during the course of this research. This research was supported in part by NSF, Contract No. DMR9202176.

[1] M. C. Bost and J. E. Mahan, J. Appl. Phys. **58**, 2696 (1985).
[2] N. E. Christensen, Phys. Rev. B **42**, 7148 (1990).
[3] J. E. Mahan, K. M. Geib, G. Y. Robinson, R. G. Long, Y. Xinghua, G. Bai, M-A. Nicolet, and M. Nathan, Appl. Phys. Lett. **56**, 2126 (1990).
[4] J. Chevrier, V. Le Thanh, S. Nitsche, and J. Derrien, Appl. Surf. Sci. **56-58**, 438 (1992).
[5] H. Moritz, B. Rosen, S. Popovic, A. Rizzi, and H. Luth, J. Vac. Sci. Technol. B **10**, 1704 (1992).
[6] D. Gerthsen, K. Rademacher, Ch. Dieker, and S. Mantl, J. Appl. Phys. **71**, 3788 (1992).
[7] H. Sirringhaus, N. Onda, E. Muller-Gubler, P. Muller, R. Stalder, and H. von Kanel, Phys. Rev. B **47**, 10567 (1993).
[8] M. G. Grimaldi, P. Baeri, C. Spinella, and S. Logamarsino, Appl. Phys. Lett. **60**, 1132 (1992).
[9] C. H. Olk, O. P. Karpenko, G. L. Doll, J. F. Mansfield, and S. M. Yalisove (unpublished).
[10] P. Tiwari, M. Bahtnagar, R. Dat, and J. Narayan, Mater. Sci. Eng. B **14**, 23 (1992).
[11] J. T. Cheung and H. Sankur, CRC Critical Rev. Solid State Mater. Sci. **15**, 63 (1988).
[12] G. L. Doll, *The 1993 McGraw Hill Yearbook of Science and Technology* (McGraw–Hill, New York, 1993), pp. 198–200.
[13] F. J. Grunthaner and P. J. Grunthaner, Mater. Sci. Rep. **1**, 65 (1986).
[14] R. A. Neifeld, S. Gunapala, G. Liang, S. A. Shaheen, M. Croft, J. Price, D. Simmons, and W. T. Hill, III, Appl. Phys. Lett. **53**, 703 (1988).
[15] J. Lash, C. H. Ching, R. M. Gilgenbach, and G. L. Doll (unpublished).
[16] L. Reimer, *Transmission Electron Microscopy*, 3rd ed. (Springer, Berlin, 1993), pp. 359–361.